Three Dimensional Posture Control of Mono-wheel Robot with Roll Rotatable Torso

Yasutaka Fujimoto
Department of Electrical and Computer Engineering
Yokohama National University
Yokohama 240-8501 Japan
Email: fujimoto@ynu.ac.jp

Shuhei Uchida
Department of Electrical and Computer Engineering
Yokohama National University
Yokohama 240-8501 Japan
uchida@fujilab.dnj.ynu.ac.jp

***Abstract*— This paper presents three dimensional stabilization of a monowheel robot that has a roll axis joint at the waist part of the robot and a wheel. The robot is under actuated system. The robot in sagittal plane approximates a pendulum on a cart. The robot in lateral plane approximates a double pendulum whose first axis is under actuated. This robot has only two actuators and is supposed to be the minimum structure of the mobile robot. In this paper, the motion equation of the system is derived. Then, stabilizing controllers for sagittal and lateral motion are presented. Through the three dimensional simulation where whole three dimensional dynamics is considered, the validity of the controller is verified. Moreover, in combination of sagittal and lateral controller, turning motion around yaw axis is realized in spite of lack of a yaw axis actuator.**

I. Introduction

Recent years, many studies for wheel-type mobile robots have been reported. Most of them have two actuated wheels and some passive wheels. When the robot turns quickly, it receives the cornering centrifugal force. Let the mass of the robot be M, the linear velocity of the robot be v, the angular velocity around the yaw axis be ω. Then the centrifugal force is represented by $F = Mv\omega$. In the case of a two-wheel robot, it is limited within a certain value depending on the structure of the robot. The condition is given by $|F| \leq gd/h$, where g is the gravity acceleration, d is a half length of the tread, and h is the height of the center of mass. Thus, the tread of the two-wheel robot has to be designed widely in order to achieve quick motion.

On the other hand, a few studies for one actuated wheel robots have been reported in [1] and [2]. The monowheel robots are expected to become a low-cost but high-mobility platform for mobile robots. Moreover, a monowheel robot has interesting properties from the viewpoint of control theory. The system is instable and has to stabilize three dimensional posture, i. e., pitching, rolling, and yawing motions by using a few actuators. These motions are nonlinearly coupled each other. In the past work, a monowheel robot with actuators for pitching motion and yawing motion that generates a gyro effect is proposed[1].

This paper presents three dimensional stabilization of a mono-wheel robot that has a roll axis joint at the waist part of the robot and a wheel. The robot is under actuated system. The robot in sagittal plane approximates a pendulum on a cart. The robot in lateral plane approximates a double pendulum whose first axis is under actuated. Although the system is hard to stabilize, the robot requires only two actuators. This robot is supposed to be the minimum structure of the mobile robot. The cost of the robot is expected less than other mobile robots. There is no past work regarding mono-wheel robot that has only two actuators. In this paper, the motion equation of the system is derived. Then, stabilizing controllers for sagittal and lateral motion are presented. Through the three dimensional simulation where whole three dimensional dynamics is considered, the validity of the controller is verified. Moreover, in combination of sagittal and lateral controller, turning motion around yaw axis is realized in spite of lack of a yaw axis actuator.

The rest of the paper is organized as follows. In Section II, a model of a monowheel robot is introduced where the lateral and sagittal motion is represented. The design of stabilizing controller for both lateral and sagittal motion is explained in the Section III, The three dimensional numerical simulation of the monowheel robot is provided in Section IV, and introduction of an experimental setup is introduced in Section V. Conclusions are outlined in the Section VI.

II. Model of Monowheel Robot

A. A Model of Monowheel Robot in Lateral Plane

In this paper, a model of the monowheel robot in the lateral plane is equivalent to a double inverted pendulum whose first joint is underactuated as shown in Fig. 1. Only a waist joint is the input for rolling motion. Parameters of the model are shown in Table I.

The motion equation of the model is obtained as follows.

$$\dot{x_l} = \begin{bmatrix} \dot{\theta}_l \\ M_l(\theta_l)^{-1}\left(\tau_l - h_l(\theta_l, \dot{\theta}_l) - G_l(\theta_l)\right) \end{bmatrix} \tag{1}$$

where

$$M_l(\theta_l) = \begin{bmatrix} I_1 + I_2 + m_2(\ell_1^2 + 2\ell_1 r_2 c_2) & I_2 + m_2\ell_1 r_2 c_2 \\ I_2 + m_2\ell_1 r_2 c_2 & I_2 \end{bmatrix} \tag{2}$$

$$h_l(\theta_l, \dot{\theta}_l) = \begin{bmatrix} -m_2\ell_1 r_2 s_2(2\dot{\theta}_1\dot{\theta}_2 + \dot{\theta}_2^{\,2}) + D_1\dot{\theta}_1 \\ m_2\ell_1 r_2 s_2\dot{\theta}_1^{\,2} + D_2\dot{\theta}_2 \end{bmatrix} \tag{3}$$

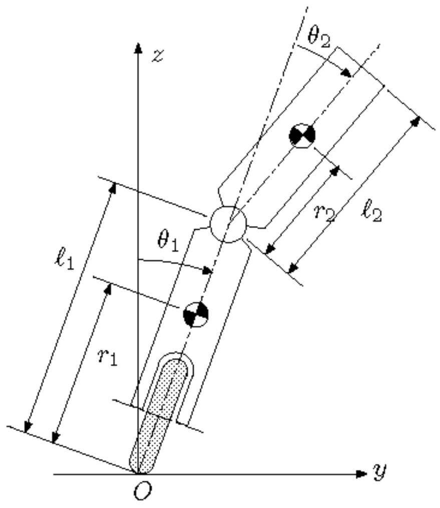

Fig. 1. A model of the monowheel robot in lateral plane.

TABLE I
PARAMETERS OF THE MONOWHEEL ROBOT IN LATERAL PLANE.

length of i-th link	ℓ_i [m]
mass of i-th link	m_i [kg]
angle of 1st link	θ_1 [rad]
angle of waist joint	θ_2 [rad]
input torque for waist joint	τ_2 [N.m]
position of center of mass of i-th link	r_i [m]
inertia of i-th link	I_i [kg m^2]
damping factor of i-th axis	D_i [N.m s/rad]
gravity acceleration	g [m/s^2]
centrifugal acceleration	g_2 [m/s^2]

$$G_l(\theta_l) = -g \begin{bmatrix} (m_1 r_1 + m_2 \ell_1) s_1 + m_2 r_2 s \\ m_2 r_2 s \end{bmatrix} + g_2 \begin{bmatrix} (m_1 r_1 + m_2 \ell_1) c_1 + m_2 r_2 c \\ m_2 r_2 c \end{bmatrix} \tag{4}$$

Other notations are $s_i = \sin\theta_i$, $c_i = \cos\theta_i$, $s = \sin(\theta_1+\theta_2)$, $c = \cos(\theta_1+\theta_2)$, $\theta_l = [\theta_1, \theta_2]^T$, $\tau_l = [0, \tau_2]^T$, and $x_l = [\theta_1, \theta_2, \dot\theta_1, \dot\theta_2]^T$.

Linearizing the nonlinear motion equation (1) around equilibrium point $\theta_1 = \tan^{-1}(g_2/g)$, $\dot\theta_1 = \theta_2 = \dot\theta_2 = 0$, the following linear system is obtained.

$$\dot{x}_l = A_l x_l + B_l \tau_2 \tag{5}$$

$$y_l = C_l x_l \tag{6}$$

where

$$A_l = \begin{bmatrix} 0 & 1 & 0 & 0 \\ a_{21} & a_{22} & a_{23} & a_{24} \\ 0 & 0 & 0 & 1 \\ a_{41} & a_{42} & a_{43} & a_{44} \end{bmatrix} \tag{7}$$

$$B_l = \begin{bmatrix} 0 \\ -(I_2 + m_2 \ell_1 r_2)/S_l \\ 0 \\ (I_1 + I_2 + m_2 \ell_1^2 + 2 m_2 \ell_1 r_2)/S_l \end{bmatrix} \tag{8}$$

$$C_l = \begin{bmatrix} 0 & 0 & 1 & 0 \\ 0 & 1 & 0 & 0 \end{bmatrix} \tag{9}$$

and

$$a_{21} = \frac{1}{S_l}\sqrt{g^2+g_2^2}\left(I_2(m_1 r_1 + m_2 \ell_1) - m_2^2 \ell_1 r_2^2\right)$$

$$a_{22} = -\frac{D_1 I_2}{S_l}$$

$$a_{23} = -\frac{1}{S_l}\sqrt{g^2+g_2^2} m_2^2 \ell_1 r_2^2$$

$$a_{24} = \frac{D_2(I_2 + m_2 \ell_1 r_2)}{S_l}$$

$$a_{41} = \frac{1}{S_l}\sqrt{g^2+g_2^2}(m_2 r_2 (I_1 - \ell_1(m_1 r_1 - m_2 r_2)) - I_2(m_1 r_1 + m_2 \ell_1))$$

$$a_{42} = \frac{D_1(I_2 + m_2 \ell_1 r_2)}{S_l}$$

$$a_{43} = \frac{1}{S_l}\sqrt{g^2+g_2^2}(m_2 r_2 (I_1 + m_2 \ell_1^2 + m_2 \ell_1 r_2)$$

$$a_{44} = \frac{-D_2(I_1 + I_2 + m_2 \ell_1^2 + 2 m_2 \ell_1 r_2)}{S_l}$$

$$S_l = I_2(I_1 + m_2 \ell_1^2) - m_2^2 \ell_1^2 r_2^2$$

In the linearized representation, order of the state variable is modified as $x_l = [\theta_1, \dot\theta_1, \theta_2, \dot\theta_2]^T$.

TABLE II
PARAMETERS OF THE MONOWHEEL ROBOT IN SAGITTAL PLANE.

position of robot	x [m]
inclination angle of robot	θ_3 [rad]
rotation angle of wheel	ϕ [rad]
damping factor for linear motion	D_x [N s/m]
damping factor for wheel axis	D_θ [N.m s/rad]
input torque for wheel axis	τ_1 [N.m]
mass of wheel	m_w [kg]
inertia of wheel	I_w [kg m^2]
combined inertia of two links	I_3 [kg m^2]
radius of wheel	r [m]

B. A Model of the Monowheel Robot in Sagittal Plane

A model of the monowheel robot in the sagittal plane is equivalent to a inverted pendulum on a cart as shown in Fig. 2. Parameters of the model are shown in Table II.

Assume that there is no slip between wheel and ground. The linear position of the robot x is represented by using the rotation angle of the wheel ϕ and the inclination angle of the robot θ_3.

$$x = r(\phi - \theta_3) \tag{10}$$

The motion equation of the robot in sagittal plane is given by

$$\dot{x}_s = \begin{bmatrix} \dot\theta_s \\ M_s^{-1}(\theta_s)\left(\tau_s - h_s(\theta_s, \dot\theta_s) - G_s(\theta_s)\right) \end{bmatrix} \tag{11}$$

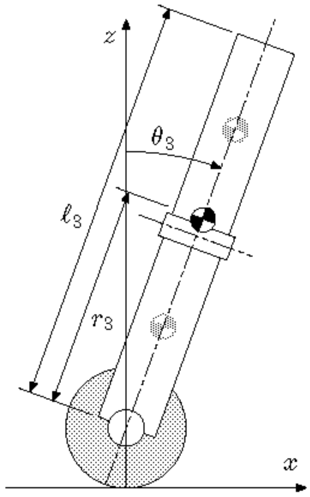

Fig. 2. A model of the monowheel robot in sagittal plane.

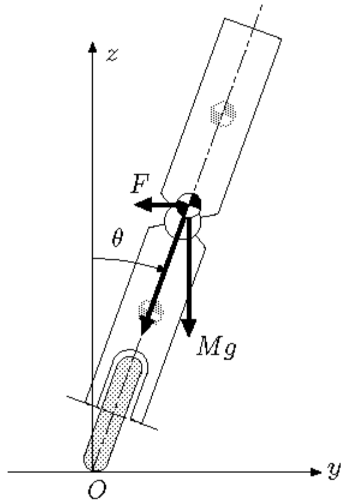

Fig. 3. A model for turning control.

where

$$M_s(\theta_s) = \begin{bmatrix} m + m_3 + I_3/r^2 & m_3\ell_G c_3 \\ m_3\ell_G c_3 & I_3 + m_3{\ell_G}^2 \end{bmatrix} \quad (12)$$

$$h_s(\theta_s, \dot{\theta}_s) = \begin{bmatrix} D_x\dot{x} - m_3 s_3 \ell_G {\dot{\theta}_3}^2 \\ D_\theta \dot{\theta}_3 \end{bmatrix} \quad (13)$$

$$G_s(\theta_s) = \begin{bmatrix} 0 \\ -m_3 g \ell_G s_3 \end{bmatrix} \quad (14)$$

Other notations are as follows: $\theta_s = [x, \theta_3]^T$, $\tau_s = [\tau_1, 0]^T$, $m_3 = m_1 + m_2$, $\ell_G = (m_1 r_1 + m_2(\ell_1 + r_2))/m_3$, and $x_s = [x, \theta_3, \dot{x}, \dot{\theta}_3]^T$.

Linearizing the nonlinear motion equation (11) around equilibrium point $x = \dot{x} = \theta_3 = \dot{\theta}_3 = 0$, the following linear system is obtained.

$$\dot{x}_s = A_s x_s + B_s \tau_1 \quad (15)$$

$$y_s = C_s x_s \quad (16)$$

where

$$A_s = \begin{bmatrix} 0 & 1 & 0 & 0 \\ 0 & k_{22} & k_{23} & k_{24} \\ 0 & 0 & 0 & 1 \\ 0 & k_{42} & k_{43} & k_{44} \end{bmatrix} \quad (17)$$

$$B_s = \begin{bmatrix} 0 \\ \frac{r^2(I_3 + m_3{\ell_G}^2}{S_s} \\ 0 \\ \frac{-m_3 r^2 \ell_G}{S_s} \end{bmatrix} \quad (18)$$

$$C_s = \begin{bmatrix} 1/r & 0 & 1 & 0 \\ 0 & 0 & 0 & 1 \end{bmatrix} \quad (19)$$

and

$$k_{22} = -\frac{1}{S_s} r^2 D_x (I_3 + m_3 {\ell_G}^2)$$

$$k_{23} = -\frac{g m_3^2 r^2 {\ell_G}^2}{S_s}$$

$$k_{24} = \frac{m_3 r^2 D_\theta \ell_G}{S_s}$$

$$k_{42} = \frac{D_x m_3 r^2 \ell_G}{S_s}$$

$$k_{43} = \frac{1}{S_s} g m_3 \ell_G ((m_w + m_3) r^2 + I_w)$$

$$k_{44} = -\frac{1}{S_s} D_\theta ((m_w + m_3) r^2 + I_w)$$

$$S_s = I_3((m_w + m_3)r^2 + I_w) + m_3(m_w r^2 + I_w){\ell_G}^2$$

In the linearized representation, order of the state variable is modified as $x_s = [x, \dot{x}, \theta_3, \dot{\theta}_3]^T$

C. Turning Motion Around Yaw Axis

The robot receives the cornering centrifugal force F during turning motion as shown in Fig. 3. When the robot moves with linear velocity $\dot{x}$ and yawing angular velocity ω, the radius R of turning motion is uniquely determined by the following equation.

$$\dot{x} = R\omega \quad (20)$$

Therefore, the centrifugal force F is represented by

$$F = MR\omega^2 = M\dot{x}\omega \quad (21)$$

where M is the total mass of the robot.

In order to balance the robot against the centrifugal force, the robot needs to incline toward the inside. From Fig. 3, the angle of inclination θ balance at the following condition.

$$\tan\theta = \frac{\dot{x}\omega}{g} \quad (22)$$

III. Design of Controller

A. Lateral Controller

It is not easy to dynamically measure the inclination angle of the robot. In our experimental setup, angular velocities of first link around pitch, roll, and yaw axis are measured by gyroscopes. Also the joint angle between first link and second link and rotation angle of wheel with respect to the first link are measured by rotary encoders.

In the lateral plane, $\dot{\theta}_1$ and θ_2 are measurable. The linearized system becomes observable, thus other state variables are estimated by a minimum order observer designed for the system (5) and (6). At the same time, input disturbance d_l is estimated and used for disturbance cancellation. Also the state feedback controller is designed so as to stabilize the lateral motion around equilibrium point. The structure of the lateral control system is shown in Fig. 4.

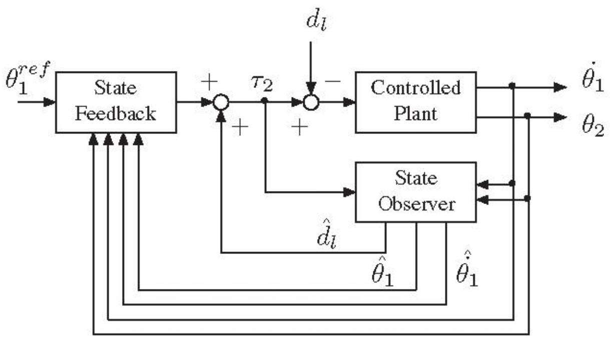

Fig. 4. Control system for lateral motion

B. Sagittal Controller

In the sagittal plane, measurements are a pitching angular velocity of the body $\dot{\theta}_3$ and a wheel rotation angle ϕ. The linear position of the robot x, the wheel rotation angle ϕ, and the inclination angle θ_3 satisfy the condition (10). Thus the output equation is represented by (19). This linearized system is also observable, thus state variables are estimated by a minimum order observer designed for the system (15) and (16). Also the input disturbance d_s is estimated and used for disturbance cancellation. The state feedback controller stabilizes the sagittal motion around equilibrium point. The structure of the sagittal control system is shown in Fig. 5.

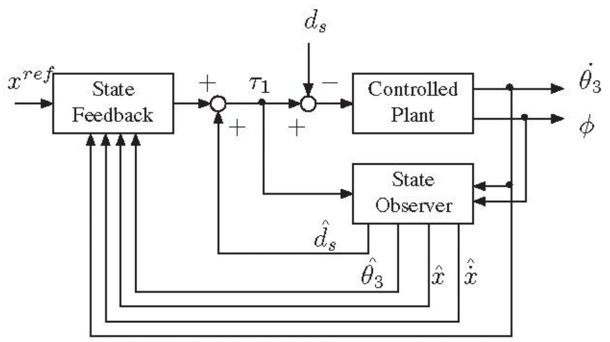

Fig. 5. Control system for sagittal motion

C. Yaw Rotation Controller

The yaw rotation controller is designed based on the condition (22). The inclination angle of the first link is determined by

$$\theta_1^{ref} = \tan^{-1}\left(\frac{\dot{x}^{ref}\omega^{ref}}{g}\right) \tag{23}$$

where $\dot{x}^{ref}$ represents the desired linear velocity of the robot and ω^{ref} represents the desired yaw axis angular velocity.

IV. Three-Dimensional Dynamical Simulation

In order to verify the validity of the proposed control system, three dimensional precise dynamical simulator[3][4] is adopted. The simulation is based on the multi-body dynamics and includes all nonlinear effects and a contact phenomenon between the wheel and the ground.

A. Posture Stabilization

Fig. 6 shows response of the posture of the robot. The initial state were set as $\theta_1 = 0.05$, $\theta_2 = 0.0$, and $\theta_3 = 0.1$. It is shown that the posture is stabilized well.

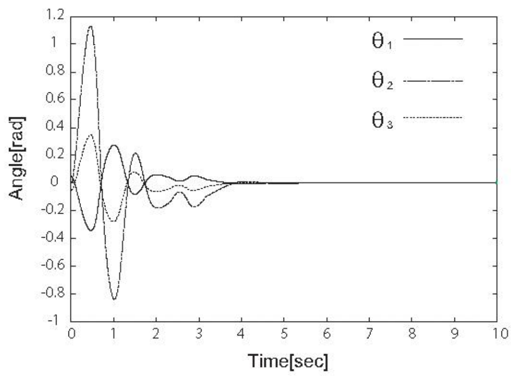

Fig. 6. Simulation result of initial response.

B. Turning Control

The turning control proposed in the previous section is verified. The reference of yaw axis angular velocity ω^{ref} in (23) is given by $\omega^{ref} = \dot{x}/R$ for $t \geq 5.0$[s] where R is the radius of the turning motion. Fig. 7 shows the linear velocity of the monowheel robot. It is shown that the actual velocity tracks the reference velocity 0.15[m/s]. Fig. 8 shows the posture of the robot. While the inclination angle of the center of mass (θ_G) follows the reference angle of the first link (θ_1^{ref}), the actual angle of the first link (θ_1) and joint angle (θ_2) have offsets. Fig. 9 shows the trajectory of the robot in the x-y plane. It is shown that the turning control is successfully achieved.

V. Development of Monowheel Robot

We have developed an actual monowheel robot as shown in Fig. 10 for the purpose of the verification of the proposed control system. The specification of the robot is shown in Table III. Most of parts are made by duralumin. The robot is equipped with Lithium-ion batteries and has a capability to move autonomously.

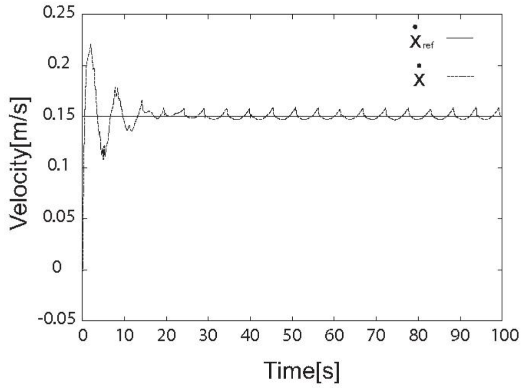

Fig. 7. Velocity of the robot

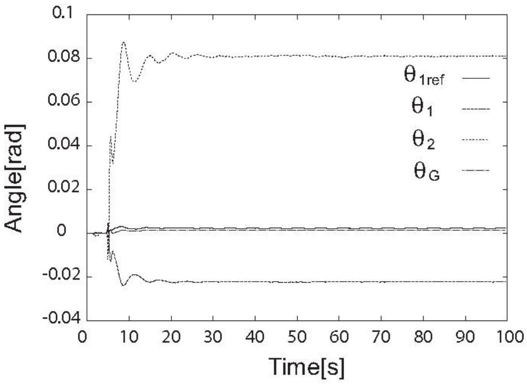

Fig. 8. Posture angle of the robot in lateral plane

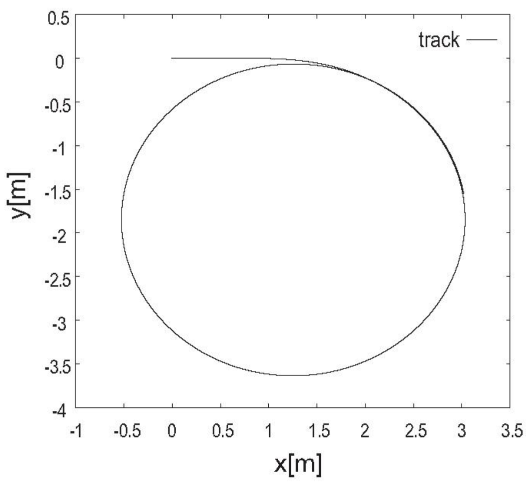

Fig. 9. Trajectory of the robot.

TABLE III

SPECIFICATION OF THE DEVELOPED MONOWHEEL ROBOT.

height	0.87 [m]
width	0.095 [m]
depth	0.25 [m]
weight	14 [kg]

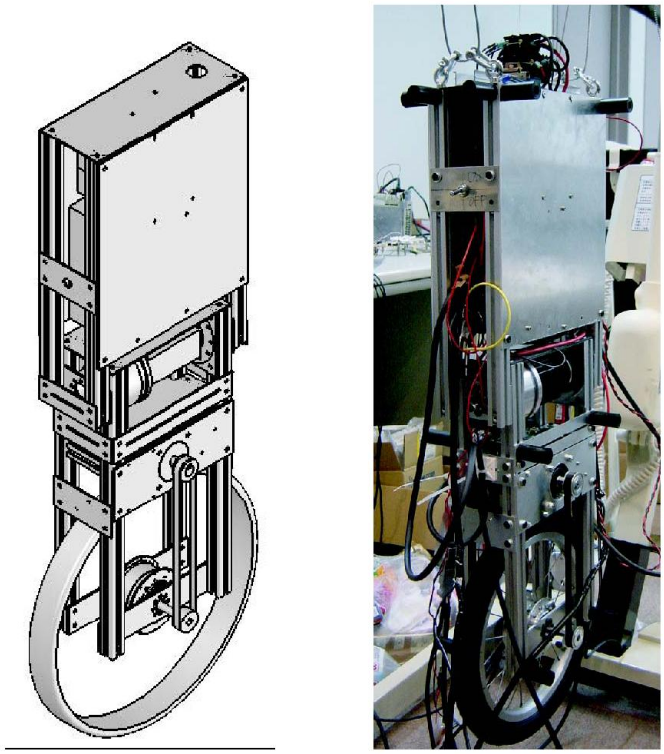

Fig. 10. Detailed drawing and a developed monowheel robot.

VI. CONCLUSION

In this paper, we have proposed three dimensional stabilization of a monowheel robot that has a roll axis joint at the waist part of the robot and a wheel. Although the monowheel robot is underactuated system, the proposed control achieves three dimensional posture stabilization including yaw axis turning motion through the three dimensional precise simulation.

For the future work, we will verify our controller by the developed experimental monowheel robot.

REFERENCES

[1] Zaiquan Sheng, and Kazuo Yamafuji, "Postural Stability of a Human Riding a Unicycle and Its Emulation by a Robot," *IEEE Trans. on Robotics and Automation*, vol. 13, no. 5, pp. 709-720, 1997.

[2] D. V. Zenkov, A. M. Bloch, and J. E. Marsden, "Stabilization of the Unicycle with Rider," *Proc. IEEE Conf. on Decision and Control*, pp. 3470–3471, 1999.

[3] Yastaka Fujimoto and Atsuo Kawamura, "Three Dimensional Digital Simulation and Autonomous Walking Control for Eight-Axis Biped Robot," *Proc. IEEE Int. Conf. on Robotics and Automation*, pp. 2877–2884, 1995.

[4] Yasutaka Fujimoto and Atsuo Kawamura, "Simulation of an Autonomous Biped Walking Robot Including Environmental Force Interaction," *IEEE Robotics and Automation Magazine*, vol. 5, no. 2, pp. 33–42, 1998.